About underappreciated, yet active conformations of thiourea organocatalysts

– *Supporting Information* –

Adriana Supady,[†] Stefan Hecht,[‡] and Carsten Baldauf*[,†]

†*Fritz-Haber-Institut der Max-Planck-Gesellschaft, Faradayweg 4-6, D-14195 Berlin, Germany*

‡*Department of Chemistry, Humboldt-Universität zu Berlin, Brook-Taylor-Str. 2, D-12489 Berlin, Germany*

E-mail: baldauf@fhi-berlin.mpg.de

Methods

Conformational searches and energy hierarchies

Conformational searches for conformers of **1**, **5**, **6**, **7** (see Figure S2) were performed by a thorough genetic-algorithm (GA) conformational search with Fafoom.[1,2] Structure searches were performed directly at the first-principles level utilizing the PBE functional[3] with a pairwise correction for long-range van der Waals interactions[4] implemented in the FHI-aims code.[5] The structures resulting from sampling of the potential-energy surface (PES) were further assessed:

- Geometry optimization were performed with the PBE0 hybrid functional[6] augmented by a many-body dispersion (MBD) correction[7] using tight species defaults.[5]

- In addition, structures were also optimized with Orca[8] utilizing the PBE[3] and PBE0[6] functionals with D3 dispersion correction,[9] cc-pVTZ basis set[10] and tight SCF convergence criteria. These calculations were performed *in vacuo* and in dichloromethane modeled as continuum utilizing the COSMO solvent model.[11]

- For comparison, MP2 optimizations with ORCA were performed in two steps: (i) first, the geometries were optimized with cc-pVTZ basis set and (ii) subsequently, single-point energy calculations with extrapolated basis set (3,4 extrapolation to the CBS limit) were performed.[12]

- For the Gibbs energies at 298.15 K, harmonic vibrational frequencies of the thiourea-derived molecules were calculated numerically:

  - The values plotted in Figure S2 were computed *in vacuo* using the PBE0+D3 hybrid functional with an increment of 0.005 bohr for the numerical integration.

  - The Gibbs energy values discussed in the manuscript and shown here in Tables S1 to S5 contain the potential energy at the PBE0+D3 level of theory in dichloromethane with a free energy correction computed with the D3 dispersion corrected PBE functional again considering dichloromethan as COSMO continuum solvent. The increment for the numerical integration was set to 0.0075 bohr in order to avoid small non-zero frequencies.

  .

- Boltzmann ratios were calculated according to equation 1 at a temperature of $298.15K$ with $R = 0.001987 kcal/(molK)$:

$$\frac{N_i}{N_{total}} = \frac{e^{-\Delta G_i/RT}}{\sum_{k=1}^{N_{total}} e^{-\Delta G_k/RT}} \tag{1}$$

Computational details on the modeling of the Diels-Alder reaction

In the simulated reaction, we consider the *cis* conformer of dienophile **2** and the *endo* product **4**. The simulation of the forward reaction involved multiple steps:

1. Geometry optimization of the isolated reactants **2** and **3** as well as the product **4** utilizing dispersion-corrected PBE functional.

2. Search for the most stable arrangement for the reactant **2** together with the different conformers (*syn-syn*, *syn-anti*, *anti-anti*) of the catalyst **1** utilizing dispersion-corrected PBE functional.

    - Search for the most stable pose of **1** (*anti-anti*) and **2**: 20 random placements of **2** around the catalyst **1** satisfying following constraint: both distances between the oxygen of **2** and the N-bound hydrogens of the catalyst **1** are in range 1.5-2.3 Å. The energetically most stable pose was selected for further considerations.
    - Search for the most stable pose of **1** (*syn-anti* or *syn-syn*) and **2**: 40 random placements of **2** around the catalyst **1** satisfying following constraint: at least of the distances between the oxygen of **2** and the N-bound hydrogens of the catalyst **1** is in range 1.5-2.3 Å. In the case of *syn-syn*, the most stable pose was selected for further considerations. In the case of *syn-anti* the most stable as well as a further pose were selected for further considerations. The additionally selected pose is the most stable pose among poses, where the reactant **2** is placed on the same side as the sulfur atom of **1**.

3. To the most stable poses of the reactant **2** together with the different conformers of **1**, the reactant **3** was placed manually in a close distance and relaxed to final state of the reaction, i.e. the catalyst and product **1**+**4**. The initial state of reaction, i.e. the catalyst and the reactants **1**+**2**+**3**, was simulated by dragging away the reactant **3** from reactant **2** and a subsequent relaxation.

4. Having obtained the initial and final states of the reactions, the transition state search was performed. The transition states were found with the growing string method[13] as implemented in aimsChain.[14]

5. All steps of the reaction were subject to a refinement with the ORCA program package,[8] employing the D3 dispersion corrected PBE functional[3,9] with and without the COSMO solvation model.[11] The initial and final steps of the reactions were optimized to the corresponding minima while the transition states were subject to eigenvector-following transition state optimizations for verification.

Supplementary results

Validity of the applied level of electronic structure theory

For three MP2-optimized conformers of **1**, we calculated energies using the domain-based local pair natural orbital (DLPNO) CCSD(T) method.[15,16] Calculation were performed with Ahlrichs' def2-SVP, def2-TZVPP, and def2-QZVPP basis sets.[17] A three-point scheme for the independent extrapolation of SCF[18] and correlation energy[19] was used to extrapolate energies at the complete basis-set (CBS) limit. A more detailed description of the method can be found in the article by Ropo *et al.*[20]

The resulting energy hierarchy is compared to energies obtained with the PBE and PBE0 functionals with and without Grimme's D3 dispersion correction (with Dunning's triple-zeta basis set).

This comparison impressively shows the need for applying dispersion corrections and validates the potential-energy method used in our manuscript.

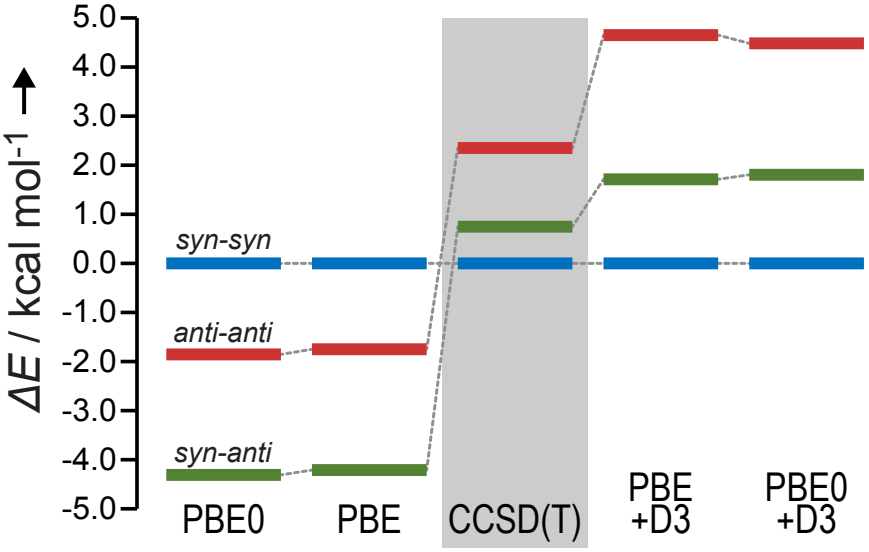

Figure S1: Potential-energy hierarchy of MP2-optimized geometries of **1** at the DLPNO-CCSD(T) level (energies extrapolated to the complete basis set limit) compared to pure and dispersion corrected PBE and PBE0 density functionals (cc-pVTZ basis).

Conformational preferences of thiourea-derived molecules

The results of conformational searches for the molecules **1**, **5**, **6**, **7** are summarized in Figure S2. The results obtained with the two different dispersion correction schemes did not differ significantly.

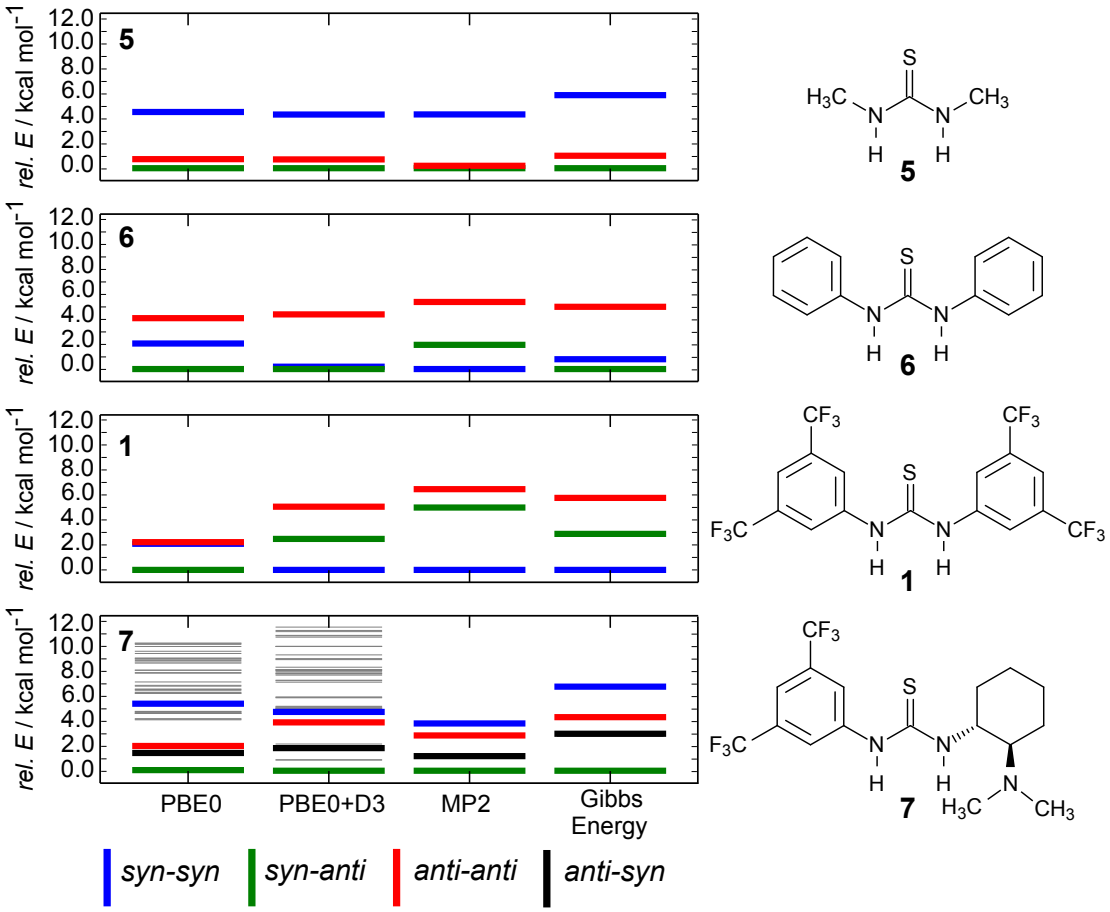

Figure S2: Chemical structures of catalyst **1** and of three related molecules. Molecule **7** is known as Takemoto catalyst along with relative energies at different levels of theory: PBE0, PBE0+D3, MP2. In the last column, the Gibbs energy calculated at the PBE0+D3 level at 298.15 K is shown. Due to the two different substituents, **7** can adopt two distinct *anti-syn* and *syn-anti* conformations.

Potential and Gibbs energies of different catalyst conformations alone and with bound substrates

Table S1: Relative potential energies (gas phase) and Gibbs energies (in dichloromethane) (in kcal/mol) of catalyst molecule **1**, ΔG values are plotted in Figure 1 of the manuscript.

Conf.	ΔE_{pot}	ΔG
syn-syn	0.00	0.00
TS1	9.24	8.50
syn-anti	3.58	3.06
TS2	11.17	11.84
anti-anti	3.84	3.51

Table S2: Relative potential energies (gas phase) and Gibbs energies (in dichloromethane) (in kcal/mol) of catalyst molecule **1** alone, bound to molecule **2** or bound to molecules **2** and **3**. ΔG values are plotted in Figure 2 of the manuscript.

Conf.	ΔE_{pot}	ΔG
1 *syn-syn*	0.00	0.00
1 *syn-anti*	3.58	3.06
1 *anti-anti*	3.84	3.51
1+**2** *syn-syn*	0.17	1.10
1+**2** *syn-anti* (1)	0.00	0.00
1+**2** *anti-anti*	3.87	5.27
1+**2** *syn-anti* (2)	3.70	4.06
1+**2**+**3** *syn-syn*	1.36	1.67
1+**2**+**3** *syn-anti* (1)	0.00	0.00
1+**2**+**3** *anti-anti*	1.44	1.59
1+**2**+**3** *syn-anti* (2)	4.83	6.50

Table S3: Relative potential energies (gas phase) and Gibbs energies (in dichloromethane) (in kcal/mol) of catalyst molecule **1** alone, bound to molecule **2** or bound to molecules **2** and **3**. ΔG values are plotted in Figure 2 of the manuscript.

Conf.	ΔE_{pot}	ΔG
2+**3** (no catalyst)		
initial	0.00	0.00
TS	9.65	12.32
final	-27.37	-20.99
1+**2**+**3** *anti-anti*		
initial	1.44	1.59
TS	8.40	11.72
final	-24.81	-16.79
1+**2**+**3** *syn-anti* (1)		
initial	0.00	0.00
TS	7.14	10.74
final	-27.56	-21.85
1+**2**+**3** *syn-syn*		
initial	1.36	1.67
TS	8.70	10.08
final	-24.98	-18.82
1+**2**+**3** *syn-anti* (2)		
initial	4.83	6.50
TS	12.28	15.76
final	-22.24	-15.74

Table S4: Relative potential energies (in dichloromethane, in kcal/mol) of the steps of the discussed reaction with and without catalyst computed with different functionals.

Conf.	E(PBE+D3)	E(PBE0+D3)	E(M06-2X)	E(B3LYP)	E(B3LYP+D3)
			2+**3** (no catalyst)		
initial	0.00	0.00	0.00	0.00	0.00
TS	6.68	9.65	14.13	15.77	12.78
final	-21.04	-27.37	-22.01	-12.93	-15.17
			1+**2**+**3** *anti-anti*		
inintial	1.29	1.44	2.69	0.34	1.66
TS	5.32	8.40	14.34	11.84	11.62
final	-18.62	-24.81	-18.74	-11.79	-12.32
			1+**2**+**3** *syn-anti* (1)		
initial	0.00	0.00	0.00	0.00	0.00
TS	4.38	7.14	10.77	13.46	9.87
final	-20.82	-27.51	-23.00	-13.09	-15.26
			1+**2**+**3** *syn-syn*		
initial	1.42	1.36	1.44	2.82	1.38
TS	5.93	8.70	12.93	16.17	11.59
final	-18.33	-24.98	-19.83	-10.15	-12.78
			1+**2**+**3** *syn-anti* (2)		
initial	4.66	4.83	4.92	0.14	5.52
TS	9.25	12.28	16.74	13.15	15.85
final	-15.50	-22.24	-17.44	-11.84	-9.50

HOMO and LUMO energies

The energy levels of the highest occupied molecular orbitals (HOMO) and the lowest unoccupied molecular orbitals (LUMO) were investigated at the level of hybrid functionals (PBE0) for various configurations. Results can be found in Figure S3.

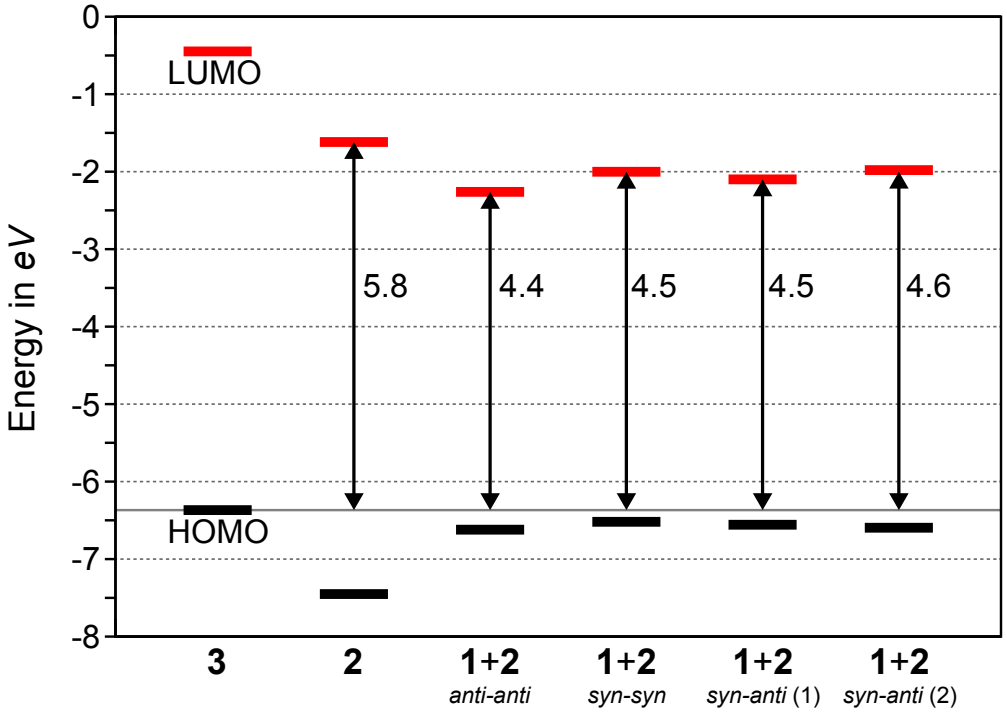

Figure S3: HOMO and LUMO energies for different configurations at the PBE0 level of theory.

Reaction rates from harmonic transition-state theory

Harmonic transition-state theory (HTST) yields the reaction rate k_{HTST} as:

$$k_{HTST} = A\ e^{-B}. \tag{2}$$

The prefactor A can be seen as an attempt frequency that is calculated as a quotient of two product series:

$$A = \frac{\prod_{i}^{3N-6} \nu_i^{Cat+S}}{\prod_{j}^{3N-7} \nu_j^{TS}}, \tag{3}$$

where ν_i^{Cat+S} are $3N-6$ normal mode frequencies of the educt state Cat+S and ν_j^{TS} are the $3N-7$ (one imaginary frequency left out) normal mode frequencies of the transition state. A comes in units of s^{-1} and can be seen as more or less constant for the reaction pathways resulting from the different Cat+S poses as well as for the uncatalyzed reaction (see values in Table S5).

The probability for overcoming the barrier, the exponential term in Equation 2 is a Boltzmann term:

$$B = (\Delta G^{TS} - \Delta G^{Cat+S})/k_B T. \tag{4}$$

$\Delta G^{TS} - \Delta G^{Cat+S}$ represents the relative barrier height $\Delta\Delta G$, essentially the activation energy. The probability of overcoming the barrier e^{-B} can differ by a factor of ten among the catalyst geometries and results in the differing reaction rates shown in Table S5.

Table S5: Characteristics for the different reaction pathways based on harmonic transition-state theory.

Conf.	A in $10^9\,s^{-1}$	e^{-B}	k_{HTST} in s^{-1}	$\Delta\Delta G$ in kcal mol^{-1}
no cat	19.1	$1.1 \cdot 10^{-9}$	20.4	12.32
anti-anti	15.4	$4.1 \cdot 10^{-8}$	638.2	10.13
syn-anti (1)	5.3	$1.5 \cdot 10^{-8}$	80.0	10.74
syn-syn	5.8	$7.4 \cdot 10^{-7}$	4279.2	8.41
syn-anti (2)	2.2	$1.8 \cdot 10^{-7}$	394.8	9.26

Structures available for download

The Cartesian coordinates (in *xyz* format) as well as the Orca outputs of the numerical harmonic frequency calculations (PBE+D3 in COSMO dichloromethane) of selected structures:

- Catalyst **1** in *syn-syn*, *syn-anti*, and *anti-anti* conformation as well as the transition states *TS1* and *TS2*,
- Substrates **2** and **3** alone,
- Catalyst **1** and substrate **2** in *syn-syn*, *syn-anti*(1), *syn-anti*(2), and *anti-anti* conformation,
- Initial and transition state of catalyst **1** and substrates **2** and **3** in *syn-syn*, *syn-anti*(1), *syn-anti*(2), and *anti-anti* conformation, and
- Final state of catalyst **1** and products **4** in *syn-syn*, *syn-anti*(1), *syn-anti*(2), and *anti-anti* conformation

are available for download here:

`http://w0.rz-berlin.mpg.de/user/baldauf/data/ASupady_Output_Coords.zip`.

References

(1) Supady, A.; Blum, V.; Baldauf, C. *J. Chem. Inf. Model.* **2015**, 2338–2348.

(2) Supady, A. Fafoom - Flexible algorithm for optimization of molecules. `https://github.com/adrianasupady/fafoom`.

(3) Perdew, J. P.; Burke, K.; Ernzerhof, M. *Phys. Rev. Lett.* **1996**, *77*, 3865–3868.

(4) Tkatchenko, A.; Scheffler, M. *Phys. Rev. Lett.* **2009**, *102*, 073005.

(5) Blum, V.; Gehrke, R.; Hanke, F.; Havu, P.; Havu, V.; Ren, X.; Reuter, K.; Scheffler, M. *Comput. Phys. Commun.* **2009**, *180*, 2175–2196.

(6) Adamo, C.; Barone, V. *J. Chem. Phys.* **1999**, *110*, 6158.

(7) Ambrosetti, A.; Reilly, A. M.; DiStasio, R. A.; Tkatchenko, A. *J. Chem. Phys.* **2014**, *140*, 18A508.

(8) Neese, F. *WIREs: Comput. Mol. Sci.* **2012**, *2*, 73–78.

(9) Grimme, S.; Antony, J.; Ehrlich, S.; Krieg, H. *J. Chem. Phys.* **2010**, *132*, 154104.

(10) Dunning, T. H. *J. Chem. Phys.* **1989**, *90*, 1007.

(11) Klamt, A.; Schüürmann, G. *J. Chem. Soc., Perkin Trans. 2* **1993**, 799.

(12) Neese, F.; Valeev, E. F. *J. Chem. Theory Comput.* **2011**, *7*, 33–43.

(13) Peters, B.; Heyden, A.; Bell, A. T.; Chakraborty, A. *J. Chem. Phys.* **2004**, *120*, 7877–7886.

(14) Yao, Y.; Supady, A.; Baldauf, C.; Scheffler, M.; Ghiringhelli, L. M. *in prep.*

(15) Riplinger, C.; Neese, F. *J. Chem. Phys.* **2013**, *138*, 034106.

(16) Riplinger, C.; Sandhoefer, B.; Hansen, A.; Neese, F. *J. Chem. Phys.* **2013**, *139*, 134101.

(17) Weigend, F.; Ahlrichs, R. *Phys. Chem. Chem. Phys.* **2005**, *7*, 3297–305.

(18) Karton, A.; Martin, J. M. L. *Theor. Chem. Acc.* **2006**, *115*, 330–333.

(19) Truhlar, D. *Chem. Phys. Lett.* **1998**, *294*, 45–48.

(20) Ropo, M.; Schneider, M.; Baldauf, C.; Blum, V. *Sci. Data* **2016**, *3*, 160009.